A BUCK-BOOST TRANSFORMERLESS INVERTER FOR 1- GRID-CONNECTED SOLAR PV SYSTEMS

RONDI BABU[1]RUHEENA BEGUM[2]BUCHALA AKANKSHA[3] RASAMALLA RAKESH KUMAR[4] CHINTALA SUPRADEEPA[5]

[1]Associate professor, Department of EEE, Jyothismathi institute of technology and science, Nustulapur, Karimnagar, TS, India

[2,3,4,5]UG students, Department of EEE, Jyothismathi institute of technology and science, Nustulapur, Karimnagar, TS, India

Abstract: For single-phase grid-connected solar PV applications, this study introduces a revolutionary single-stage buck-boost transformerless inverter topology (BBTI). As a result of this topology, there are no leakage currents in this system, which makes it ideal for use with solar panels. A buck-boost capability allows the suggested design to follow the maximum power point even when the input PV voltage fluctuates widely. Additionally, the suggested topology uses only one energy storage inductor that offers symmetric operation on both half cycles of the grid. According to the suggested topology, two of its five switches run at line frequency, which results in minimal switching losses, while the other three conduct in any mode of operation that incurs low conductions losses. The proposed inverter topology is evaluated and presented in detail using a simple sine-triangle pulse width modulation technique. The 300W laboratory prototype was used for simulations, and the results demonstrate that the proposed system has a greater efficiency and lower THD in the output current than the current system.

Keywords: Leakage currents, Pulse width modulation, and Buck-boost converter.

I.INTRODUCTION

Leakage currents are common in PV-fed. transformerless inverters [1]. There are several PV-fed transformerless inverter topologies and control solutions that have been developed to overcome the leakage currents [2] and [3]. Examples include grid-connected central or string inverter systems, which do not require a boost stage for strings of PV panels. Low-voltage PV sources, on the other hand, necessitate a boost stage, reducing the system's efficiency. The buck generated transformerless inverters may not work when the PV source is low voltage or when the PV source is shadowed. [4, 5]. An inverter without transformers and buck-boost capability is recommended for extensive operation of PV sources [6–16]. As a result of this, buck-boost based topologies [10]-[15] have become more popular among researchers in recent years. For a variety of PV systems, buck-boost inverter topologies have been developed by the authors in [10]. In addition, this design requires two distinct PV sources for each half-cycle of the output voltage. Using only four power switches and two input inductors, [11] proposes a transformerless buck-boost topology. DC current injection can occur in this design because each input inductor runs in either a positive or negative half cycle. This topology also has the problem of having a THD in current that exceeds IEEE regulations by more than 5%. Using a single input inductor and five switches, the authors in [12] developed a buck-boost derived design as well. However, this design requires three additional diodes. Even though this topology only has one input inductor, it still requires a big input capacitor to track the maximum power from the PV source. The poor voltage gain of this design is another drawback. There are a variety of PV systems that can benefit from the architecture in [13]. But eight power switches and a single inductor are required for this. Adding more switches affects efficiency and reliability while also raising the overall system cost. The number of switches in [14]'s buck-boost derived topology is reduced (i.e. five switches). A greater input capacitance is needed to track the maximum point of solar PV in this architecture. PV systems of all sizes can benefit from the topology shown in [14]. Three switches are in use during each switching cycle in this design, resulting in higher conduction losses. Because this system requires a high current capability

inductor, it increases system size and costs and affects efficiency. This is a drawback. Researchers in [15] developed a buck-boost architecture with only two power switches in order to further minimize the switch's count. However, this design does not perform symmetrically in both the positive and negative half cycles of the output voltages. Additionally, the voltage across the input PV must be greater than what is required for output. Using a linked inductor, another topology was proposed [16]. A significant output voltage gain can be achieved with this configuration;however, three power switches are active at the same time, increasing conduction losses and lowering efficiency. A buck-boost transformer less inverter design with only five power switches and a single input inductor is proposed in this work in light of the aforementioned drawbacks. The following are the main advantages of the proposed topology: One of the advantages of using a common terminal is that there is no leakage current between the PV and the grid. The symmetry of operation in both the positive and negative half-cycles result in a negligible injection of DC current. The system is more dependable and efficient because there are fewer programmable switches. Due to buck-boost functioning, a wide range of PV power tracking is possible.

II. PROPOSED SYSTEM

Buck-boost transformer less inverter topology and modes of operation are discussed in this section.

a) The Buck-Boost transformer less inverter topology's structure

To illustrate this new transformerless inverter (BBTI) design, we present Fig. 1. Combining a buck-boost DC-DC converter and a full-bridge inverter yields this BBTI topology, one power diode, one input inductor (L), and one auxiliary capacitor (CA) make up the BBTI's five programmable switches S1 to S5. High frequency (i.e., switching frequency) is used by switches S1, S3, and S4; line frequency is used by switches S2, and S5 (i.e., 50Hz). Leakage currents are fully eliminated when the PV's negative terminal is directly linked to the grid's neutral in the BBTI architecture depicted in Fig. 1. According to the continuous conduction mode, the BBTI's operating modes are depicted in Figs. 2(a)-(d) and their associated switching states are shown in Table-I in the case of iL>0 grid voltage.

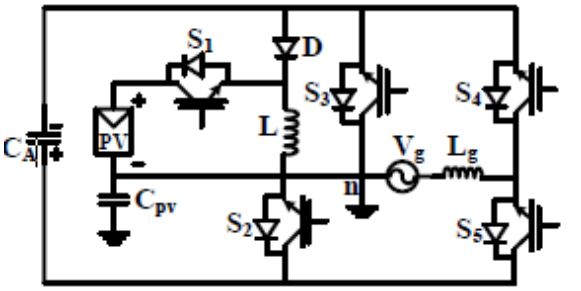

Figure 1.A buck-boost transformerless inverter (BBTI) topology

TABLE I :SWITCHING STATES IN OPERATING MODES

Operation of BBTI		Switches states (1=ON, 0=OFF)						Mode
		S_1	S_2	S_3	S_4	S_5	D	
+Ve half cycle	i_L>0	1	0	1	0	1	0	a
		0	0	0	0	1	1	b
-Ve half cycle		1	1	0	1	0	0	c
		0	1	0	0	0	1	d

b) Operating modes

Mode-(a) to Mode-(d) of the BBTI's continuous conduction mode corresponds to the grid's positive and negative half cycles. Positive half cycles of the grid are represented by mode-(a), mode-(b), mode-(c), mode-(d) (Figs. 2(a), (b, d) respectively). Table I shows the various switching states for all modes of operation. Here are the BBTI's modes of operation for the four most important modes of operation:

As illustrated in Fig. 2, in mode-(a) the BBTI provides electricity to the grid during this mode' (a). With S1 and S3 off, and all three of the power switches selected, the system will operate normally. There are two power switches, S1 and S3, that allow for power storage in the inductor (L), and S3 and S5 provide electricity to the grid. With this mode of operation indicated in Fig. 2, all of the current-flowing routes are marked with thick lines (a).

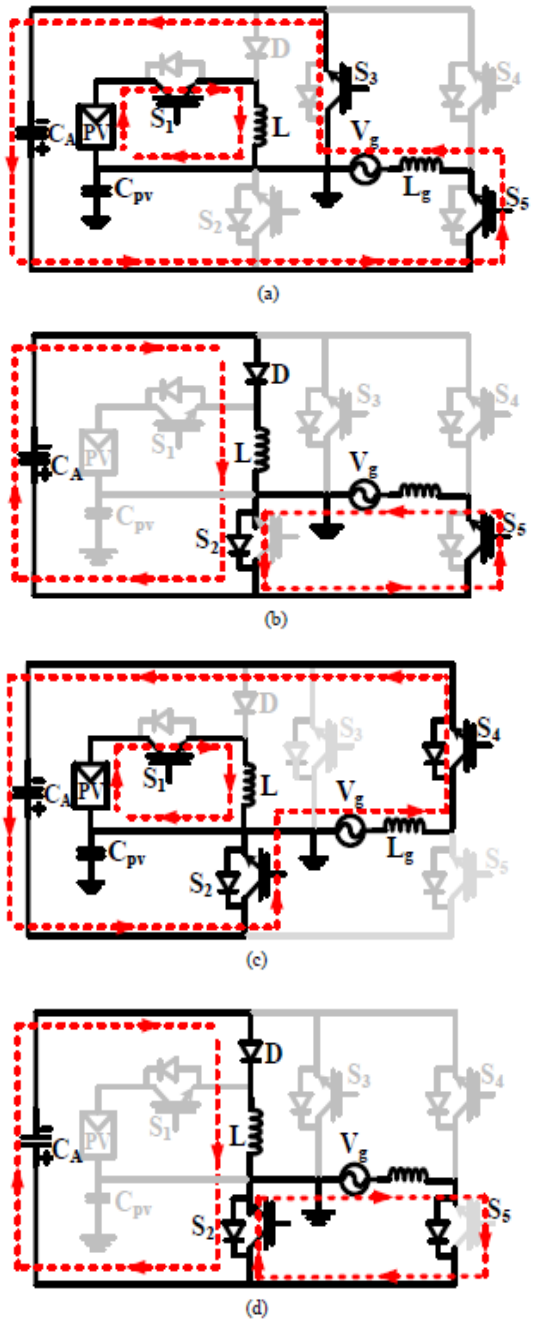

Fig. 2 illustrates the buck-boost transformerless inverter's many modes of operation. There are four modes of operation available: (a) Mode-(a): Powering mode; (b) Mode-(b): Freewheeling mode; (c) Mode-(c): Powering mode in the negative half cycle; and (d) Mode- (d): Freewheeling mode in the negative half cycle.

Operators can switch to mode-(b) by pressing and holding down the power switch while the other switches are turned off (Fig. 2 shows this way of operation) (b). The auxiliary capacitor CA receives power from the inductor (L) via a diode (D) and an anti-parallel diode (S2) in parallel. Inductor 'Lg' freewheels through switch S5 and the anti-parallel diode of switch S2 in the grid. With this mode of operation, all conductive pathways are marked with thick lines as seen in Fig. 2. (b). the negative half cycle of powering the grid is represented by mode (c). The power switches S1, S2, and S4 are all switched on during this mode. Power is supplied to the grid via the auxiliary capacitor CA via power switches S2 and S4. Switch S1 connects the energy storage inductor to the PV source. Thin lines denote conductor pathways associated with this mode of operation, as depicted in Figure 2. (c). In Mode-(d), Inductor Lg's freewheeling period is represented by this mode. While the other power switches are switched off, the power switch is remained on. Through diodes D and S2's anti-parallel diode, inductor 'L' delivers its stored energy to the auxiliary capacitor CA. Switch S2 and anti-parallel diode of switch S5 freewheel the current in the inductor Lg. According to this manner of operation, thick lines are drawn on all the conductors, as illustrated in Fig. 2. (d).

III. PROPOSED CONTROL SYSTEM

Grid-connected BBTI has modulation and control mechanisms described here.

A. BBTI topology modulation and control techniques

Fig. 3 depicts the BBTI topology's proposed modulation approach. There are three waves that are compared in this modulation strategy: the modulating waveform, the modulating waveform's inverse (-Vmsin(wt)), and its absolute (|Vmsin(wt)|).

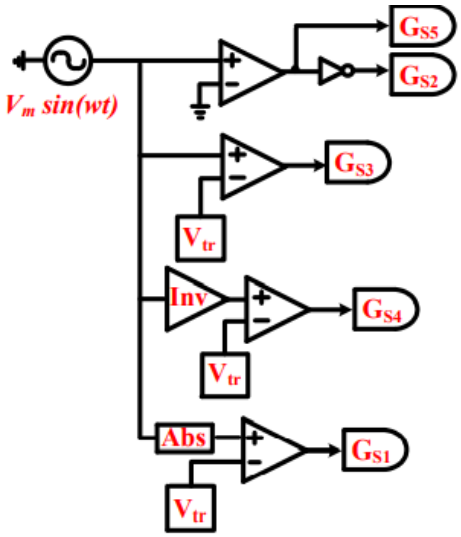

Fig. 3. The BBTI topology's proposed modulation scheme.

switching pulses to the switches are generated using a triangular waveform (Vtr) (S1 to S5). As depicted in Figure 3, the switches S2 and S5 operate at line frequency (i.e. 50Hz). To generate the S3 switching pulse, Vmsin(wt) is compared to a triangle waveform (Vtr). It is similarly formed by comparing Vtr with the triangular waveforms |Vmsin(wt)| and -Vmsin(wt)|. The present control approach is used to feed electricity from the input PV source to the grid in the proposed BBTI topology [11]. The perturb and observe MPPT algorithm [7] is used to track the input solar PV source's maximum power point.

B. Findings from an evaluation of existing transformerless inverter topologies to compare the new design with those already in use

As demonstrated in Figure 2(a)-(d), the proposed BBTI topology incurs lower switching and conduction losses since only three switches operate at high frequency and only three switches conduct during any mode of operation. Due to its lower switching and conduction losses, the BBTI topology is more efficient than current transformerless inverter topologies. According to the Table-II, the thorough comparison of the proposed BBTI topology with the existing transformerless inverter topologies is provided.

TABLE II COMPARISON OF BBTI WITH OTHER BUCK-BOOST TRANSFORMERLESS INVERTER TECHNOLOGIES

Parameters	BBTI	Ref [11]	Ref [13]	Ref [15]
Number of switches	5	6	5	5
Number of diodes	1	0	2	0
Number of inductors	1	1	2	1
Number of capacitors	1	1	0	1
DC offset	No	No	Yes	Yes
% THD	3.31	<5	<5	4.5

IV. SIMULATION RESULTS

TABLE III SIMULATION STUDIES SYSTEM CHARACTERISTICS

Power rating	300W
Switching frequency	10kHz
Input voltage	75V
Input inductor (L)	115µH
Auxiliary capacitor(C_A)	50 µF
Output inductor (L_g)	1mH
Filter capacitor (C_f)	10 µF

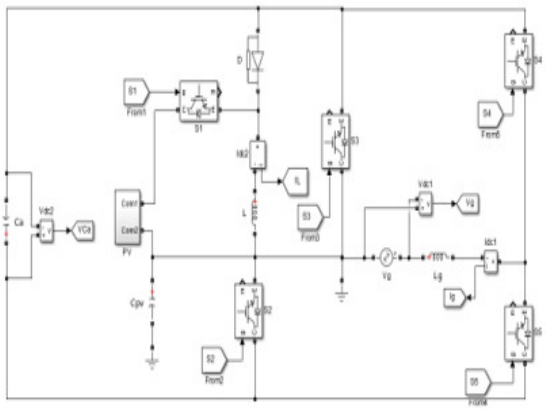

Fig.4 MATLAB/SIMULINK circuit diagram of the proposes BBTI

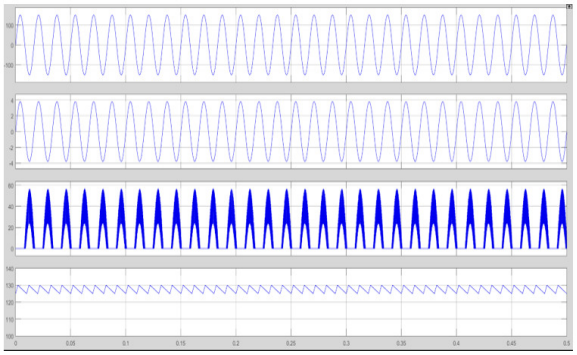

Fig. 5. The grid voltage (Vg), grid current (Ig), input inductor current (iL), and voltage across an auxiliary capacitor are all shown in the simulated waveforms for the PV-fed grid-connected BBTI system (VCA)

CONCLUSION

A unique buck-boost transformerless inverter topology was proposed, studied and proven by experimental results. It has been verified that the BBTI topology injects 0% leakage current and negligible DC current into the grid for grid-connected PV application. Due to the buck-boost property of the BBTI the maximum power point can be tracked for PV under the large voltage variation. The BBTI was tested at the switching frequency of 10 kHz and it has been observed that the THD in current is 3.8 percent which is in good agreement with the IEEE specifications.

REFERENCES

[1] E. Gubia, P. Sanchis, A. Ursua, J. Lopez, and L. Marroyo, "Ground currents in single-phase transformerless photovoltaic systems," in Progress in Photovoltaics: Research and Applications. New York: Wiley, pp. 629-650, Nov. 2007. [2] Gubía. E, Sanchis. P, Ursúa. A, López. J and Marroyo. L, “Ground currents in single-phase transformerless photovoltaic systems,” in Progress in Photovoltaics: Research and Applications. NewYork: Wiley, pp. 629- 650, 2007.

[3] O. Lopez et al. “Eliminating ground current in a transformerless photovoltaic application,” IEEE Trans. on Energy Conversion, vol. 25, no. 1, pp. 140–147, Mar. 2010.

[4] D. Barater, E. Lorenzani, C. Concari, G. Franceschini, and G. Buticchi, “Recent advances in single-phase transformerless photovoltaic inverters,” IET Renew. Power Gener., vol. 10, no. 2, pp. 260–273, 2015.

[5] W. Yu, 1. S. Lai, H. Qian, C. Hutchens, J. Zhang, G. Lisi, A. Diabbari, G. Smith and T. Hegarty, "High-efficiency inverter with H6-type configuration for photovoltaic non-isolated AC module applications," Proc. IEEE Appl. Power Electron. Conf. Expo., pp.1056 -1061, Feb. 2010.

[6] N. Kasa, H. Ogawa, T. Iida, and H. Iwamoto, “A transformerless inverter using buck-boost type chopper circuit for the photovoltaic power system,” in Proc. IEEE Int. Conf. Power Electron. Drive Syst., 1999, pp. 653–658.

[7] S. Jain and V. Agarwal, “A single-stage grid-connected inverter topology for solar PV systems with maximum power point tracking,” IEEE Trans. Power Electron., vol. 22, no. 5, pp. 1928–1940, Sep. 2007.

[8] B. S. Prasad, S. Jain, and V. Agarwal, “Universal single-stage gridconnected inverter,” IEEE Trans. Energy Convers., vol. 23, no. 1, pp. 128–137, Mar. 2008.

[9] H. Patel and V. Agarwal, "A single-stage, single-phase transformerless doubly grounded grid-connected PV interface," IEEE Trans. Energy Conversion, vol. 24, pp. 93–101, Mar. 2009.

[10] Y. Tang, X. Dong, and Y. He, “Active buck-boost inverter,” IEEE Trans. Ind. Electron., vol. 61 no. 9, pp. 4691–4697, Sep. 2014.

[11] P. Chamarthi, M. Rajeev, and V. Agarwal, “A novel single-stage zero leakage current transformerless inverter for grid-connected PV systems,” in Proc. IEEE 42nd Photovolt. Spec. Conf., New Orleans, LA, USA, Jun. 2015, pp. 1–5.

[12] N. V´azquez, M. Rosas, C. Hern´andez, E. V´azquez, and F. J. Perez-Pinal, “A new common-mode transformer-less PV inverter,” IEEE Trans. Ind. Electron., vol. 62, no. 10, pp. 6381–6391, Oct. 2015.

[13] T. Sreekanth, N. Lakshminarasamma, and M. K. Mishra, “A single-stage grid-connected high gain buck-boost inverter with maximum power point tracking,” IEEE Trans. Energy Convers., vol. 32, no. 1, pp. 330–339, Mar. 2017.

[14] A. Kumar and P. Sensarma, “A four-switch single-stage single-phase buck-boost inverter,” IEEE Trans. Power Electron., vol. 32, no. 7, pp. 5282–5292, Jul. 2017.
[15] V. Gautam and P. Sensarma, “Design of Cuk-derived transformer-less common-grounded PV micro-inverter in

CCM," IEEE Trans. Ind. Electron., vol. 64, no. 8, pp. 6245–6254, Aug. 2017.

[16] T. Sreekanth, N. Lakshminarasamma, and M. K. Mishra, "A single-stage grid-connected high gain buck-boost inverter with maximum power point tracking," IEEE Trans. Energy Convers., vol. 32, no. 1, pp. 330–339, Mar. 2017.